Design of a Protein Surface Antagonist Based on α-Helix Mimicry: Inhibition of gp41 Assembly and Viral Fusion**

Justin T. Ernst, Olaf Kutzki, Asim K. Debnath, Shibo Jiang, Hong Lu, and Andrew D. Hamilton*

The design of low molecular weight ligands (< 750 Da) that disrupt protein – protein interactions has remained a challenging endeavor.[1] Conventional means of identifying small molecules from chemical libraries that are inhibitors of protein – protein interactions have resulted in limited success.[2] Therefore, new strategies focusing on the rational design of molecules that recognize protein surfaces could prove fruitful in the development of novel antagonists. Herein we describe such a strategy based on the design of a molecular scaffold that mimics the surface of an α-helix. We have designed a proteomimetic of an α-helical 4-3 hydrophobic repeat that inhibits the assembly of a six-helix bundle corresponding to the fusion-active conformation of the gp41 protein.[3] This intraprotein surface disruption results in reduced levels of HIV-1 entry into host cells.

The gp41 ectodomain contains an N-terminal glycine-rich fusion sequence, as well as two helical regions containing hydrophobic 4 – 3 heptad (*abcdefg*) repeats denoted as the N- and C-helical regions (N and C refer to regions situated towards the N- and C-terminus, respectively, Figure 1). Recent evidence has shown that gp41 undergoes a conformational change upon binding target surface cell receptors which exposes the hydrophobic N-helical regions and allows the fusion peptides to insert into the host cell membrane.[4] This transient gp41 intermediate then refolds into a stabilized six-helix bundle structure, which brings both the viral and target cell membranes into proximity and results in completion of the fusion process. The fusion-critical helix bundle has been shown by X-ray diffraction data to exist as a gp41 trimer in which the N-helical regions form a parallel trimeric coiled coil and the C-helical regions subsequently pack in an antiparallel fashion into the hydrophobic grooves formed by the coiled coil (Figure 1).[3a]

Antagonists that bind the exposed N-helical regions of the transient gp41 intermediate can potentially trap this structure prior to bundle formation, which leads to inhibition of viral fusion.[3a, 5] Peptides with sequences corresponding to the C-helical region of gp41 are potent inhibitors of HIV fusion,[6] one of which is currently in human trials.[7] Small molecules that bind into a hydrophobic pocket in the N-helical trimer inhibit viral fusion in vitro, with activities in the low micromolar range.[2b, 8] However, other sites along the hydrophobic grooves of the N-helical trimer are also important for recognition of the C-helical region,[3a, 9] as evidenced by the strong binding of C-terminal peptides that lack the key Trp residues (W_{628} and W_{631} in gp41).[6b, 10] Also, small peptides corresponding to the pocket binding region have negligible viral fusion inhibition and mutations of C-terminal peptide residues distant from the W_{628} and W_{631} binding region abolish inhibition activity.[11, 12] These results suggest that a small molecule mimetic of the helical 4 – 3 hydrophobic repeats could bind multiple sites along the coiled coil of the N-helical region, and disrupt formation of the helix bundle.

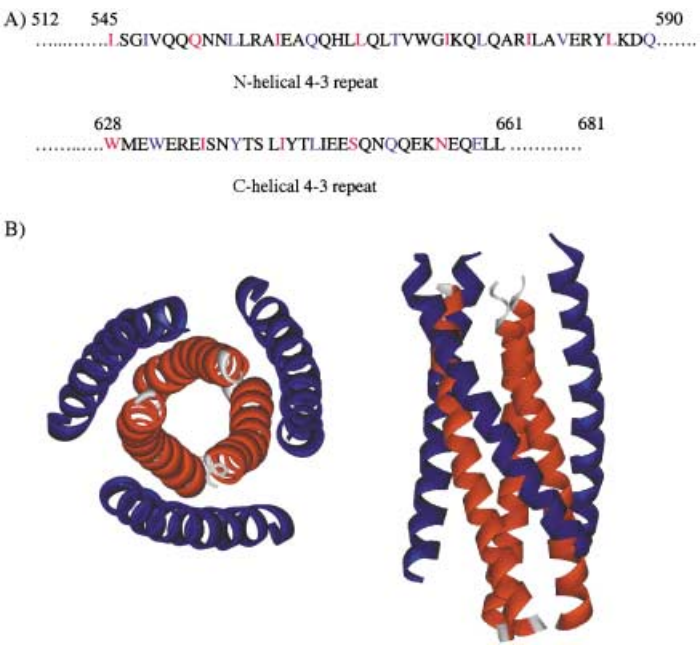

Figure 1. A) Sequences of the gp41 ectodomain corresponding to the helical 4 – 3 repeat regions (aa 545 – 590 and 628 – 661). The residues colored in red and blue correspond to the *a*- and *d*-positions, respectively, in the heptad repeat. B) Top and side views of the crystal structure of the fusion active core of gp41. The helices correspond to the N36 (red, aa 546 – 581) and the C34 peptides (blue, aa 628 – 661).

Trisfunctionalized 3,2′,2″-terphenyl derivatives serve as effective mimics of the surface functionality projected along one face of an α-helix.[13] To target the gp41 complex we prepared terphenyl derivative **1a**, which mimics the side chains of an i, $i+4$, $i+7$ *dad* hydrophobic surface, as found in the heptad repeat regions of the C- and N-peptides. Although there are a range of hydrophobic residues at the *a*- and *d*-positions (Figure 1), Leu and Ile are the most prevalent. Therefore, we have incorporated the related branched alkyl substituents isobutyl and isopropyl (to avoid complications from chirality in a *sec*-butyl group) into our initial design. Terminal carboxylate groups were also added to mimic the anionic character of the C-helical region of the peptide and to improve the aqueous solubility.

The low energy barrier of rotation about the phenyl – phenyl bonds in this system[14] makes an energetically mini-

[*] Prof. Dr. A. D. Hamilton, J. T. Ernst, Dr. O. Kutzki
Department of Chemistry
Yale University
P.O. Box 208107, New Haven, CT 06520-8107 (USA)
Fax: (+1) 203-432-6144
E-mail: andrew.hamilton@yale.edu
Dr. A. K. Debnath, Dr. S. Jiang, Dr. H. Lu
Biochemical Virology Lab
Lindsley F. Kimball Research Institute
New York Blood Center
310 East 67th Street, New York, NY 10021 (USA)

[**] We thank the National Institutes of Health for support of this work and the Deutsche Forschungsgemeinschaft (DFG) for a research fellowship to O.K.

Supporting information for this article is available on the WWW under http://www.angewandte.com or from the author.

  1433-7851/02/4102-0278 $ 17.50+.50/0

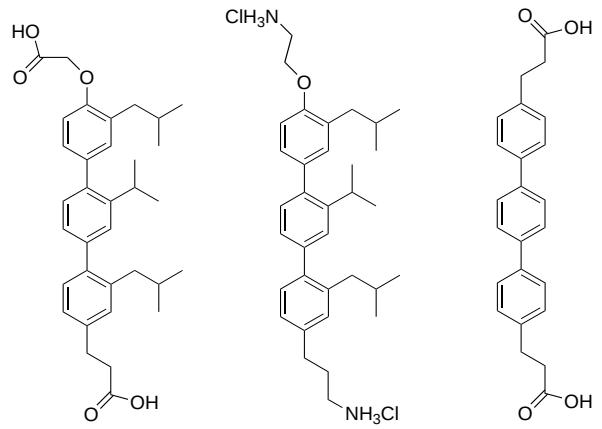

1a **2** **3**

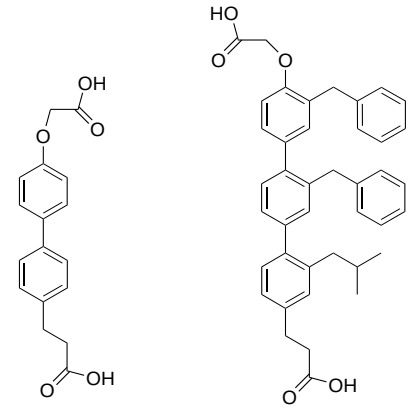

4 **1b**

mized conformation accessible that presents the phenyl substitution in a way that mimics the i, $i+4$, and $i+7$ side chains (Figure 2). Computer modeling experiments comparing a polyalanine α-helix to 3,2′,2″-trimethylterphenyl indicated that phenyl–phenyl torsion angles of 55° gave a conformation with close correspondance (root mean square deviation rmsd = 0.9 Å) of the positions of the three methyl groups and the i, $i+4$, $i+7$ alanine methyl groups (yellow in Figure 2).[15] Facile phenyl–phenyl bond rotation should allow interconversion among the conformations necessary for an induced fit upon binding to the N-peptide trimer.

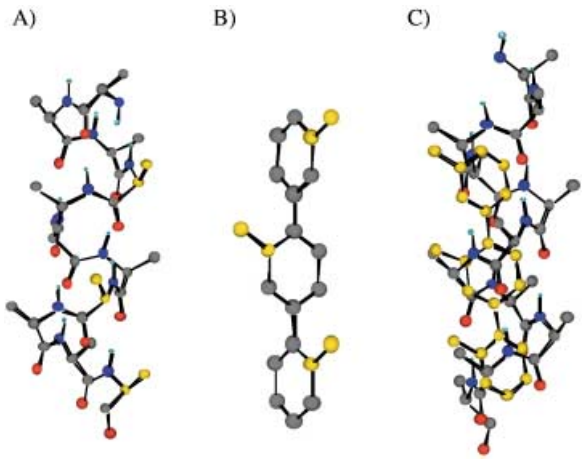

Figure 2. A) Structure of a polyalanine α-helix. B) Structure of 3,2′,2″-trimethyl terphenyl (hydrogen atoms omitted). The analogous carbon atoms between structures are highlighted in yellow. C) Root mean square difference overlay of a polyalanine α-helix and 3,2′,2″-trimethylterphenyl (yellow).

A convergent synthesis of **1a** (Scheme 1) was developed based on sequential Suzuki coupling reactions. The individual 1,4-alkoxyphenylboronate monomers could be readily prepared with different substituents at the 2-position. Compounds **2**–**4**, with opposite charge or lacking the branched alkyl sustituents, were also synthesized as controls.

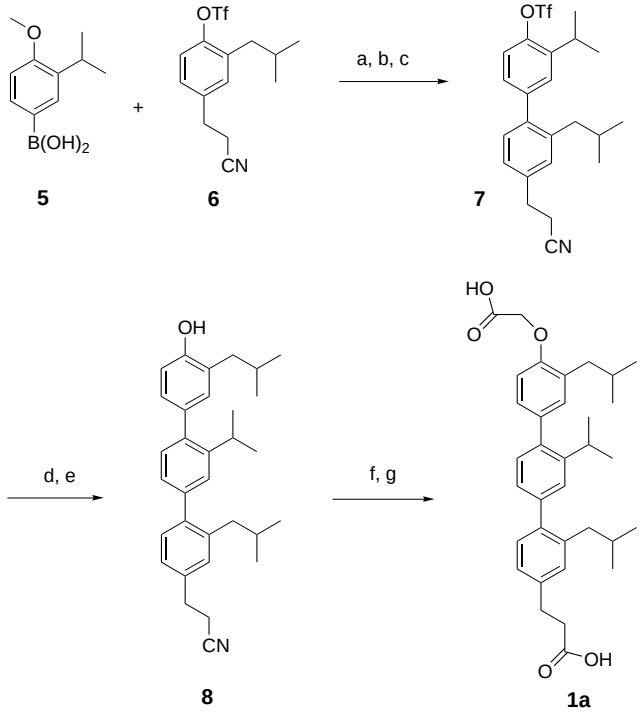

5 **6** **7** **8** **1a**

Scheme 1. a) $Pd(PPh_3)_4$, Na_2CO_3 (aq), DME/EtOH, 80 °C, 17 h, 98 %; b) BBr_3, CH_2Cl_2, 0 – 10 °C, 9 h, 92 %; c) Tf_2O, pyridine, 0 °C-RT, 17 h, 95 %; d) $Pd(PPh_3)_4$, 2-(3-isobutyl-4-methoxyphenyl)-4,4,5,5-tetramethyl-1,3,2-dioxaborolane, Na_2CO_3 (aq), DME/EtOH, 80 °C, 20 h, 87 %; e) BBr_3, CH_2Cl_2, 0 – 10 °C, 9 h, 97 %; f) CH_2ClCN, K_2CO_3, acetone, 55 °C, 40 h, 95 %; g) NaOH (aq), MeOH, 50 °C, 24 h, 74 %. DME = 1,2-dimethoxyethane, Tf = trifluoromethanesulfonyl.

The ability of **1a** to influence the disruption of the gp41 core was studied by CD spectroscopy. A model system composed of two peptides (N36 and C34), from the N- and C-heptad repeat regions of gp41, forms a stable six-helix bundle (T_m = 66 °C) that is analogous to the gp41 core (Figure 3).[3] CD experiments show that the C34 peptide alone in solution is a random coil and the N36 peptide alone forms concentration-dependent aggregates.[3b] Titration of **1a** into a 10 μM solution (50 mM phosphate-buffered saline (PBS), 150 mM NaCl, pH 7.0, 4 °C) of the preformed gp41 core model resulted in a decrease of the CD signal at Θ222 and 208 nm which corresponds to a reduction in the helicity of the hexameric bundle (Figure 3). A plot of Θ222 versus inhibitor concentration (Figure 4) shows saturation at approximately three

  1433-7851/02/4102-0279 $ 17.50+.50/0

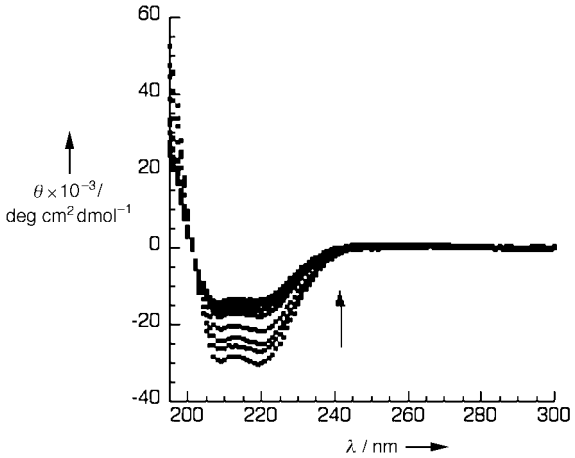

Figure 3. CD spectra of a 10 μM solution (50 mM PBS, 150 mM NaCl, pH 7.0, 4 °C) of the gp41 core model upon titration of **1a** (0–50 μM). The arrow indicates the reduction in signal at θ222 and 208 nm.

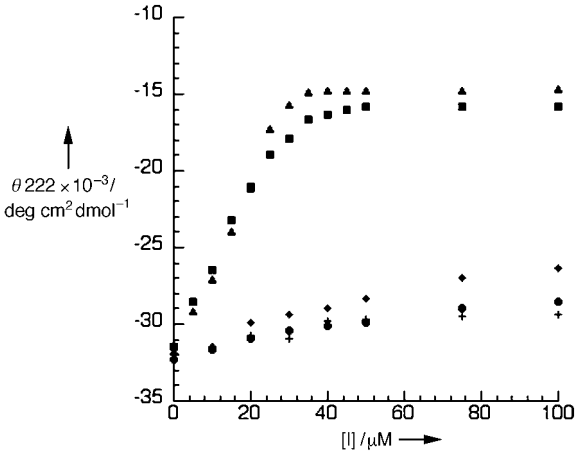

Figure 4. CD signal at θ222 nm versus inhibitor concentration: **1a** (■); **2** (◆); **3** (●); **4** (+); and **1b** (▲). The inhibitors were titrated into a 10 μM aqueous solution of the gp41 model complex (50 mM PBS, 150 mM NaCl, pH 7.0, 4 °C).

equivalents of **1a**. The CD spectrum with excess **1a** was similar to the theoretical addition of the individual N36 and C34 spectra at the same concentration.[15] The thermal denaturation curve of the gp41 core in the presence of 50 μM **1a** shows a significant drop in the T_m value (ΔT_m = 18 °C) and closely resembles the melting transition of N36 alone at the same concentration (Figure 5).[3b] These data suggest that the hexameric helix bundle structure is disrupted by helix mimetic **1a**, presumably by displacement of the C34 peptide.

Both the hydrophobic and electrostatic features of **1a** are important for its ability to disrupt the bundle. Analogues **3** and **4**, which lack the key alkyl side chains, and analogue **2**, with positively charged substituents on the hydrophobic core, have little effect on the CD spectrum of the protein even at high concentrations (Figure 4). Also, thermal denaturation experiments showed that **2**–**4** (at 100 μM) had no effect on the melting transition of the system (Table 1). To test the scope of this strategy we have increased the size of the hydrophobic substituents in **1a**, by using the bis-benzyl substituted **1b**. This molecule shows a modest enhancement in activity relative to

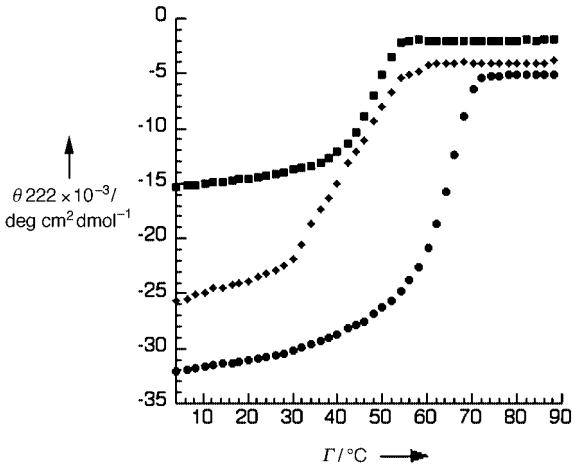

Figure 5. CD thermal denaturation experiments: 10 μM gp41 core model (●); 10 μM gp41 core model in the presence of 50 μM **1a** (■); and 10 μM N36 (◆).

Table 1. Inhibitory activities of compounds **1a**–**4**. T_m refers to the thermal melting transition of 10 μM gp41 core in the presence of inhibitor: **1a** (50 μM), **2**–**4** (100 μM).

Inhibitor	T_m [°C]	N36/C34 ELISA IC_{50} [μg mL^{-1}]	Cell Fusion IC_{50} [μg mL^{-1}]
1a	48	13.18 ± 2.54	15.70 ± 1.30.
2	65	> 100	–[a]
3	66	> 100	–[a]
4	66	> 100	–[a]

[a] No inhibition was detected below concentrations that caused cytotoxicity (~25–50 μg mL^{-1}).

1a (Figure 4), fully disrupting the hexameric bundle at a lower concentration.

The disruption of the hexameric bundle seen in the CD experiments was supported by an enzyme-linked immunosorbent assay (ELISA) for gp41 core disruption using an antibody that binds the N36/C34 helix bundle but not the individual peptides (Table 1).[16] Mimetic **1a** effectively disrupts N36/C34 complexation with an IC_{50} value of 13.18 ± 2.54 μg mL^{-1}, while **2**–**4** have no effect at 100 μg mL^{-1}.

Finally, the effects of antagonist **1a** on HIV-1 mediated fusion were studied using a dye-transfer cell fusion assay.[17] If the gp41 core is being disrupted, as implied by the CD and ELISA experiments, then the fusion mechanism of HIV-1 should be inhibited. Indeed, **1a** shows inhibition of HIV-1 mediated cell-to-cell fusion with an IC_{50} value of 15.70 ± 1.30 μg mL^{-1} (Table 1). In comparison, compounds **2**–**4** had no inhibitory activity and proved to be cytotoxic at similar concentrations (data not shown).

In conclusion, a strategy of helix mimicry based on a substituted terphenyl scaffold was applied to the design of an antagonist of gp41 core formation. CD and ELISA experiments suggest that **1a** disrupts the formation of a six-helix bundle corresponding to the gp41 fusion-active conformation, subsequently resulting in the inhibition of HIV-1 entry into host cells. The structural and mechanistic similarities of gp41 to fusion-mediating subunits of other enveloped viral glyco-

  1433-7851/02/4102-0280 $ 17.50+.50/0

proteins suggest that such a universal inhibitor design could potentially be effective against several different viruses.[18]

Received: July 16, 2001 [Z17509]

[1] For a recent review, see A. G. Cochran, *Chem. Biol.* **2000**, *7*, R85 – R94.

[2] a) A. Degterev, A. Lugovskoy, M. Cardone, B. Mulley, G. Wagner, T. Mitchison, J. Yuan, *Nat. Cell. Biol.* **2001**, *3*, 173 – 182; b) A. K. Debnath, L. Radigan, S. Jiang, *J. Med. Chem.* **1999**, *42*, 3203 – 3209; c) S. A. Qureshi, R. M. Kim, Z. Konteatis, D. E. Biazzo, H. Motamedi, R. Rodrigues, J. A. Boice, J. R. Calaycay, M. A. Bednarek, P. Griffin, Y.-D. Gao, K. Chapman, D. F. Mark, *Proc. Natl. Acad. Sci. USA* **1999**, *96*, 12156 – 12161; d) S.-S. Tian, P. Lamb, A. G. King, S. G. Miller, L. Kessler, J. I. Luengo, L. Averill, R. K. Johnson, J. G. Gleason, L. M. Pelus, S. B. Dillon, J. Rosen, *Science* **1998**, *281*, 257 – 259; e) J. W. Tilley, L. Chen, D. C. Fry, S. D. Emerson, G. D. Powers, D. Biondi, T. Varnell, R. Trilles, R. Guthrie, F. Mennona, G. Kaplan, R. A. LeMahieu, M. Carson, R. Han, C.-M. Liu, R. Palermo, G. Ju, *J. Am. Chem. Soc.* **1997**, *119*, 7589 – 7590.

[3] a) D. C. Chan, D. Fass, J. M. Berger, P. S. Kim, *Cell* **1997**, *89*, 263 – 273; b) M. Lu, P. S. Kim, *J. Bio. Mol. Struct. Dyn.* **1997**, *15*, 465 – 471.

[4] For a review, see D. C. Chan, P. S. Kim, *Cell* **1998**, *93*, 681 – 684.

[5] a) M. Lu, S. C. Blacklow, P. S. Kim, *Nat. Struct. Biol.* **1995**, *2*, 1075 – 1082; b) M. Ferrer, T. M. Kapoor, T. Strassmaier, W. Weissenhorn, J. J. Skehel, D. Oprian, S. L. Schreiber, D. C. Wiley, S. C. Harrison, *Nat. Struct. Biol.* **1999**, *6*, 953 – 960.

[6] a) S. Jiang, K. Lin, N. Strick, A. Neurath, *Nature* **1993**, *365*, 113; b) C. T. Wild, D. C. Shugars, T. K. Greenwell, C. B. McDanal, T. J. Matthews, *Proc. Natl. Acad. Sci. USA* **1994**, *91*, 9770 – 9774.

[7] a) R. A. Furuta, C. T. Wild, Y. Weng, C. D. Weiss, *Nat. Struct. Biol.* **1998**, *5*, 276 – 279; b) J. M. Kilby, S. Hopkins, T. M. Venetta, B. DiMassimo, G. A. Cloud, J. Y. Lee, L. Alldredge, E. Hunter, D. Lambert, D. Bolognesi, T. Mathews, M. R. Johnson, M. A. Nowak, G. M. Shaw, M. S. Saag, *Nat. Med.* **1998**, *4*, 1302 – 1307.

[8] D. M. Eckert, V. N. Malashkevich, L. H. Hong, P. A. Carr, P. S. Kim, *Cell* **1999**, *99*, 103 – 115.

[9] S. Jiang, A. K. Debnath, *Biochem. Biophys. Res. Commun.* **2000**, *269*, 641 – 646.

[10] D. C. Chan, C. T. Chutkowski, P. S. Kim, *Proc. Natl. Acad. Sci. USA* **1998**, *95*, 15613 – 15617.

[11] J. K. Judice, J. Y. K. Tom, W. Huang, T. Wrin, J. Vennari, C. J. Petropoulos, R. S. McDowell, *Proc. Natl. Acad. Sci. USA* **1997**, *94*, 13426 – 13430.

[12] S. Jiang, K. Lin, *Peptide Res.* **1995**, *8*, 345 – 348.

[13] B. P. Orner, J. T. Ernst, A. D. Hamilton, *J. Am. Chem. Soc.* **2001**, *123*, 5382 – 5383.

[14] K. Mislow, M. A. Glass, R. E. O'Brien, P. Rutkin, D. Steinberg, J. Weiss, C. Djerassi, *J. Am. Chem. Soc.* **1962**, *84*, 1455 – 1478.

[15] See Supporting Information.

[16] a) S. Jiang, K. Lin, L. Zhang, A. K. Debnath, *J. Virol. Methods* **1999**, *80*, 85 – 96; b) S. Jiang, K. Lin, M. Lu, *J. Virol.* **1998**, *72*, 10213 – 10217.

[17] S. Jiang, K. Lin, N. Strick, A. R. Neurath, *Biochem. Biophys. Res. Commun.* **1993**, *195*, 533 – 538.

[18] a) For a review, see J. J. Skehel, D. C Wiley, *Cell* **1998**, *95*, 871 – 874; b) P. A. Bullough, F. M. Hughson, J. J. Skehel, D. C. Wiley, *Nature* **1994**, *371*, 37 – 43; c) C. M. Carr, P. S. Kim, *Cell* **1993**, *73*, 823 – 832; d) D. Fass, S. C. Harrison, P. S. Kim, *Nat. Struct. Biol.* **1996**, *3*, 465 – 469; e) V. N. Malashkevich, D. C. Chan, C. T. Chutkowski, P. S. Kim, *Proc. Natl. Acad. Sci. USA* **1998**, *95*, 9134 – 9139; f) M. Caffrey, M. Cai, J. Kaufman, S. J. Stahl, P. T. Wingfield, D. G. Covell, A. M. Gronenborn, G. M. Clore, *EMBO* **1998**, *17*, 4572 – 4584.

A Breathing Hybrid Organic – Inorganic Solid with Very Large Pores and High Magnetic Characteristics

Karin Barthelet, Jérôme Marrot, Didier Riou,* and Gérard Férey

Porous solids[1] usually find applications in the areas of ion-exchange, separation, and catalysis. The recent discovery of new materials based upon transition metal ions[2] opens the possibility of making open frameworks that exhibit also some of the remarkable electronic properties of condensed transition metal compounds (ferro- and ferrimagnetism, metal-semiconductor transitions, ferroelectricity, combined ionic/electrical conductivity). Up to now, in the field of magnetism, the major limitation for producing porous solids with high ordering temperatures came from the structure itself. Indeed, most of the porous compounds are built from metallic clusters linked by diamagnetic linkers (phosphates, arsenates, silicates, aliphatic chains) which prevent strong, long-range interactions. To date, the highest Néel temperatures were observed for the purely inorganic porous skeleton of ULM-3[3] (37 K) and for the hybrid solid HKUST-1[4] (75 K).

To overcome this difficulty, our design strategy is to link chains of corner-sharing transition metal octahedra (which favor strong, long-range superexchange coupling) by rigid organic linkers containing delocalized π electrons for the three-dimensional transmission of the interactions. The use of such linkers was mainly developed by the groups of Yaghi and O'Keeffe,[5a] Zaworotko,[5b] and Kitagawa[5c] for metal-organic frameworks with modulable very large pores.

As an example of our design principle, we describe here the synthesis, structure, magnetic and sorption properties of a large-pore, flexible, open framework (MIL-47) that is antiferromagnetic below 95 K.

To implement this design, we used the hydrothermal reaction (teflon-lined steel autoclave Parr, four days, 473 K, autogenous pressure, filling rate: 50 %) of either a mixture of VCl_3, terephthalic acid, and desionized water (molar ratio 1:0.25:100), which only provides homogeneous pure powders, or of vanadium metal, terephthalic acid, hydrofluorhydric acid, and water (molar ratio 1:0.25:2:250) when crystals are needed. In both cases, the pH value remains 1 throughout the synthesis and the yield is close to 15 %. The resulting light yellow product, (hereafter labeled MIL-47as), which is stable in air, is formulated $V^{III}(OH)\{O_2C\text{-}C_6H_4\text{-}CO_2\}\cdot x(HO_2C\text{-}C_6H_4\text{-}CO_2H)$ ($x \sim 0.75$) on the basis of elemental analysis (calcd: C 47.1, V 14.3; found: C 46.87, V 13.79;). Both thermodiffractometry and thermal analyses (TGA2050 TA apparatus, O_2 flow, heating rate 2 K min^{-1}) show (Figure 1a) a decomposition of MIL-47as in two steps between 300 and 420 °C. The first weight loss (exp.: 32.3 %, calcd: 34.92 % for

[*] Prof. Dr. D. Riou, K. Barthelet, Dr. J. Marrot, Prof. Dr. G. Férey
Institut Lavoisier UMR CNRS 8637
Université de Versailles
St Quentin en Yvelines
45 Avenue des Etats-Unis, 78035 Versailles Cedex (France)
Fax: (+33) 1-3925-4358
E-mail: riou@chimie.uvsq.fr

  1433-7851/02/4102-0281 $ 17.50+.50/0